

**Coronary Artery Spatial Distribution, Morphology, and Composition of
Non-culprit Coronary Plaques by 64-slice Computed Tomography Angiography in
Patients With Acute Myocardial Infarction**

Akira Sato, MD,^a Hirokazu Ohigashi, MD,^b Toshihiro Nozato, MD,^b Hiroyuki Hikita,
MD,^b Mieko Tamura,^b Shinsuke Miyazaki MD,^b Yoshihide Takahashi MD,^b Taishi
Kuwahara MD,^b Atsushi Takahashi, MD,^b Michiaki Hiroe, MD,^c and Kazutaka Aonuma,
MD^a

^a Cardiovascular Division, Institute of Clinical Medicine, Graduate School of
Comprehensive Human Sciences, University of Tsukuba, Tsukuba, Japan

^b Cardiovascular Center, Yokosuka Kyosai Hospital, Yokosuka, Japan

^c Department of Cardiology, International Medical Center of Japan, Tokyo, Japan

Running title: Non-culprit coronary plaques on CTA

Address correspondence to:

Akira Sato, MD, Cardiovascular Division, Institute of Clinical Medicine,
Graduate School of Comprehensive Human Sciences, University of Tsukuba,
1-1-1 Tennodai, Tsukuba, Ibaraki 305-8575, Japan

Tel: +81-29-853-3143

Fax: +81-29-853-3143

E-mail: asato@md.tsukuba.ac.jp

Abstract

Non-invasive identification of non-culprit lesions may improve preventive strategies for acute myocardial infarction (AMI). We assessed morphology, composition, and spatial distribution of non-culprit coronary plaques in patients with AMI by computed tomography angiography (CTA). Sixty-four patients with AMI underwent 64-slice CTA within 2 week after admission, and 162 symptomatic patients with stable angina pectoris (SAP) underwent CTA and stress myocardial perfusion imaging (MPI). Of these 226 patients, 16 were excluded from analysis due to image artifacts. Mean number of non-culprit plaques per patient was 5.0 ± 2.6 in the AMI group ($n = 60$), 4.2 ± 2.6 in the SAP group with abnormal MPI ($n = 67$), and 1.1 ± 1.3 in the SAP group with normal MPI ($n = 83$) ($p < 0.01$). Positive remodeling (PR) and low-attenuation plaques (LAP) (< 30 Hounsfield Units) were more frequently observed in the AMI group (1.9 ± 1.8) than in the SAP groups (0.6 ± 0.9 in abnormal MPI, 0.2 ± 0.4 in normal MPI) ($p < 0.01$). Within the AMI group, PR and LAP was present significantly more frequently in patients with metabolic syndrome than in those without (2.6 ± 2.2 vs. 1.4 ± 1.4 ; $p = 0.03$) and was significantly more frequently distributed in the proximal segments of the left anterior descending artery ($p < 0.01$). In conclusion, 64-slice CTA may provide promising information on preventive strategies by identifying non-culprit plaque morphology and zones at high risk for future events.

Key Words: computed tomography angiography; low-attenuation plaque; positive remodeling; perfusion

The recent advent of multidetector computed tomography angiography (CTA) has greatly improved image quality and may allow more precise evaluation of coronary stenosis and plaque morphology.^{1,2} Previous CTA studies introduced the concept of noninvasive detection and characterization of coronary atherosclerotic lesions in patients with AMI and stable angina pectoris (SAP)³ and identified differences in lesion morphology and plaque composition between culprit lesions in patients with acute coronary syndrome (ACS) and stable lesions in patients with ACS or SAP.⁴ Recently, Motoyama et al. demonstrated that CT characteristics of culprit lesions in ACS included positive remodeling (PR) and low-attenuation plaques (LAP)⁵ and that patients with these 2 plaque characteristics on CTA were at a higher risk of ACS developing during follow-up when compared with patients having lesions without these characteristics.⁶ We therefore hypothesized that positively remodeled plaques with LAP in non-culprit lesions, favoring a propensity to rapidly progress to a culprit lesion or rupture, might be more frequently observed in AMI patients within the proximal third of the major epicardial coronary arteries. To investigate this hypothesis, we examined whether 64-slice CTA can noninvasively assess the spatial distribution, morphology, and composition of non-culprit lesions in patients with AMI in comparison with stable lesions in patients with SAP.

Methods

We studied a prospective but nonconsecutive series of 226 patients who underwent 64-slice CTA from September 2006 to December 2007. The study population consisted of 64 patients with AMI and 162 symptomatic patients with suspected coronary artery disease (CAD) who underwent stress myocardial perfusion imaging (MPI). In these 162 patients, stress MPI was positive in 72 patients and negative in 90 patients. AMI was defined as follows: 1) chest pain >30 minutes in duration with presentation within 12

hours after the onset of symptoms; 2) ST-segment elevation >0.1 mV within 2 contiguous electrocardiograph leads; 3) elevated creatine kinase-MB isoenzymes within 12 hours of chest pain. AMI patients underwent 64-slice CTA within 2 week after successful primary stenting. SAP was defined as no change in frequency, duration, or intensity of chest pain within 4 weeks in patients in sinus heart rhythm and without previous myocardial infarction, previous PCI or coronary bypass surgery, and unstable angina.

Of the 226 patients, 16 patients (4 in the AMI group, 5 in the SAP with abnormal MPI group, and 7 in the SAP with normal MPI group) were excluded from analysis due to image artifacts that made assessment of the entire coronary anatomy impossible on CTA images. The remaining 210 patients (AMI group, $n = 60$; SAP with abnormal MPI group, $n = 67$; SAP with normal MPI group, $n = 83$) represent the population of this study. Written informed consent was obtained from all patients, and the study protocol was approved by our institutional review board.

Scanning was performed with a 64-slice CT scanner (Aquilion 64; Toshiba Medical Systems Corporation, Otawara, Japan). According to a previous published protocol,² images were acquired with 64×0.5 -mm slice collimation, gantry rotation speed of 400 ms/rotation, table feed of 6.4 mm/gantry rotation, tube energy of 120 kV, and an effective tube current of 400 mAs. The CT dose index volume and dose-length product of this scan protocol were 75.2 mGy and 1.10 Gy•cm, respectively, and corresponded to an approximate mean radiation dose of 15 mSv. A volume of 60 ml of contrast agent (Iopamidol 370, 370 mgI/ml; Schering AG, Berlin, Germany) was injected intravenously at a rate of 4 ml/s. Patients were given oral metoprolol 20-40 mg 1 hour before the scheduled scan if their heart rate was >65 beats/min, and all patients were given sublingual nitroglycerin 0.3 mg 5 minutes before the scan.

Analysis of the scans was performed using a ZIOSTATION workstation (ZIOSOFT Inc., Tokyo, Japan). Images were initially reconstructed at 75% of the cardiac cycle with a slice thickness of 0.5 mm at an increment of 0.3 mm. In the case of motion artifacts, additional reconstructions were made at different time points of the R-R interval. Each scan was analyzed independently by 2 experienced readers who were blinded to the results of the stress Tl-201 SPECT.

The image display settings were modified on an individual basis to accommodate differences in contrast enhancement or image noise in some patients. The individually optimized window width (between 600 and 900 HU [Hounsfield Units]) and level (between 100 and 250 HU) settings were maintained for each of the measurements.⁷ Coronary atherosclerotic plaque was visually classified as follows: 1) non-calcified plaque was defined as any discernible structure that could be assigned to the coronary artery wall, with CT attenuation below that of the contrast-enhanced coronary lumen but above that of the surrounding connective tissue/epicardial fat^{7,8}; 2) calcified plaque was defined as any structure with CT attenuation of >130 HU that could be visualized separately from the contrast-enhanced coronary lumen (either because it was embedded within non-calcified plaque or because its density was above that of the contrast-enhanced lumen). Spotty calcification was defined when <3 mm in size on curved multi-planar reformation and 1-sided on cross-sectional images⁵; 3) mixed plaque was defined as plaque with non-calcified and calcified elements present; 4) LAP was defined as plaque with low CT density (<30 HU).⁶ The remodeling index (RI) was calculated by dividing the lesion diameter at the plaque site of maximum luminal narrowing by the reference diameter (proximal to the lesion in a normal-appearing vessel segment). PR was defined as a RI of >1.10. We used the coronary map modified from the

Bypass Angioplasty Revascularization Investigation (BARI).⁹ Proximal segments of coronary plaque location included #1 proximal right coronary artery (RCA), #12 proximal left anterior descending artery (LAD), and #18 proximal left circumflex (LC). Middle segments included #2 mid RCA, #13 Mid LAD, #15 diagonal 1 branches, #19 mid LC, and #20 obtuse marginal 1. Distal segments included #3 distal RCA, #4 posterior descending, #6 posterior lateral segment, #14 distal LAD, #16 diagonal 2 branches, #19a distal LCx, and #21 obtuse marginal 2.

Tl-201 SPECT was performed within 1 week of the CTA. Beta-blockers, calcium channel blockers, and nitrates were discontinued for 24-48 hours before the test. Adenosine was administered intravenously to all patients at 0.14 mg/kg/min for 6 minutes, and a dose of 111 MBq of Tl-201 was injected 3 minutes into the infusion. ECG and blood pressure were monitored before, throughout, and after the infusion. The initial image was obtained in the supine position at 5 minutes after the Tl-201 injection, and a delayed image was obtained 4 hours later.

SPECT was performed using a double-detector system (PICKER PRISM 2000XP; Shimadzu Corporation, Kyoto, Japan) equipped with a low-energy, high-resolution collimator according to a previous published protocol.² SPECT images were assessed using a 17-segment model.¹⁰ Stress and delayed images were independently analyzed by 2 nuclear medicine physicians who were blinded to the CTA data. Visual grading was defined as normal (no perfusion defects) or abnormal (stress perfusion defects with redistribution).

Hypertension was defined as blood pressure at rest $\geq 140/90$ mmHg or use of antihypertensive medication. Hyperlipidemia was defined as total fasting serum cholesterol ≥ 200 mg/dl or serum triglycerides ≥ 150 mg/dl or use of antihyperlipidemic

medication. The revised National Cholesterol Education Program criteria¹¹ define metabolic syndrome as the presence of any 3 of the following 5 traits: 1) the cut point of waist circumference was modified for Japanese as ≥ 90 cm in men and ≥ 80 cm in women according to the recommendation by the International Diabetes Federation,¹² 2) blood pressure $\geq 130/85$ mmHg or drug treatment for elevated blood pressure, 3) serum triglycerides ≥ 150 mg/dl or drug treatment for elevated triglycerides, 4) high-density lipoprotein (HDL) cholesterol < 40 mg/dl in men and < 50 mg/dl in women or drug treatment for low HDL-C, 5) fasting glucose ≥ 100 mg/dl or drug treatment for elevated blood glucose.

All data are expressed as the mean \pm SD or median and interquartile range.

Comparisons of categorical variables between groups were performed by the chi-square test or Fisher's exact test. Comparisons of continuous variables were analyzed by one-way analysis of variance or Kruskal-Wallis test. All probability values are considered significant when < 0.05 .

Results

Baseline clinical characteristics of the patients are summarized in Table 1, and characteristics of non-culprit lesions in AMI are presented in Figure 1. Of the 300 plaques identified in the AMI group, 153 (51%) plaques were classified as non-calcified, 72 (24%) as mixed, and 75 (25%) as calcified. Of the 281 plaques identified in the SAP group with abnormal MPI, 74 (26%) plaques were classified as non-calcified, 60 (22%) as mixed, and 147 (52%) as calcified. In the SAP group with normal MPI, of the 91 plaques identified, 50 (55%) were classified as non-calcified, 17 (18%) as mixed, and 25 (27%) as calcified. The mean number of coronary plaques per patient was 5.0 ± 2.6 in the AMI group, 4.2 ± 2.6 in the SAP group with abnormal MPI, and 1.1 ± 1.3 in the SAP

group with normal MPI ($p < 0.01$) (Figure 2). The mean number of PR and LAP per patient was 1.9 ± 1.8 in the AMI group, 0.6 ± 0.9 in the SAP group with abnormal MPI, and 0.2 ± 0.4 in the SAP group with normal MPI ($p < 0.01$). Of these PR and LAP, spotty calcification was observed significantly more frequently in the AMI group (0.8 ± 1.2) than in the SAP group with abnormal MPI (0.4 ± 0.7) and with normal MPI (0.03 ± 0.2) ($p < 0.01$). In the AMI group, the number of PR and LAP was significantly higher in patients with metabolic syndrome than in those without, whereas there was no difference in the total number of plaques between these two groups (Figure 3).

Spatial distribution of non-culprit coronary plaques in AMI patients on CTA images is shown in Figure 4. In the LAD and LCx coronary arteries, non-calcified, calcified, and mixed plaques were more frequently distributed in the proximal segments, whereas there were no differences in distribution of non-calcified, calcified, and mixed plaques in the RCA. PR and LAP were more frequently distributed in the proximal segments of the LAD, whereas there were no differences in distribution of PR and LAP in the RCA and LC. In the left main (LM) coronary artery, 8 (13%) plaques were classified as non-calcified, 3 (5%) as mixed, 3 (5%) as calcified, and 4 (7%) as PR and LAP. Culprit lesions in the LAD were more frequently distributed in the proximal segment (proximal 20 [55%], mid 13 [36%], distal 3 [9%], $p < 0.01$), whereas there were no differences in distribution of culprit lesions in the RCA (proximal 6 [30%], mid 8 [40%], distal 6 [30%], $p = 0.48$) and LC (proximal 2 [50%], mid 2 [50%], distal 0, $p = 1.0$).

Discussion

The major important findings of the present study are as follows. First, CT-based plaque burden is higher in AMI patients and SAP patients with abnormal MPI than in SAP patients with normal MPI. Non-culprit coronary plaque appearance mimics that of

culprit lesions. Second, in the AMI patients, the number of noncalcified plaques with low CT density and positive remodeling was significantly higher in patients with metabolic syndrome than in those without the syndrome, and these plaques were more frequently distributed in the proximal segments of the LAD. Therefore, 64-slice CTA may noninvasively provide promising information on preventive strategies by facilitating identification of coronary plaque morphology and zones at high risk for future events in AMI patients.

Approximately 6% of PCI patients will have clinical plaque progression requiring non-target lesion PCI by 1 year, and greater coronary artery disease burden confers a significantly higher risk for clinical plaque progression.¹³ With its higher X-ray output and faster tube rotation, 64-slice CTA results in high-quality, motion-free, and isotropic image quality.¹ In the present study, we showed that on CTA images, a significantly greater number of coronary plaques in non-culprit lesions is observed in AMI patients than in SAP patients with normal MPI. Non-calcified, mixed, and PR and LAP were more significantly observed in AMI patients than in SAP patients. Leber et al. found that non-calcified plaques contribute to a higher degree to total plaque burden in AMI than in SAP.³ In addition, 64-slice CTA enables the visualization of lipid cores and spotty calcifications that are frequently associated with plaque ruptures.⁷ Positive remodeling and lipid cores are associated with plaque vulnerability in both histopathologic¹⁴ and intravascular ultrasound (IVUS) studies.^{15,16} Patients demonstrating positively remodeled coronary segments with LAP on CTA are at a higher risk of ACS developing over time.⁶ The present study suggests that all 3 major coronary arteries in patients with AMI are extensively diseased and have multiple plaques that could potentially cause another occurrence of ACS, although the natural course of this plaque development and

disruption has not yet been clearly established.

Recent studies have demonstrated that metabolic syndrome is associated with an increasing risk of cardiovascular disease.¹⁷ Furthermore, IVUS study has shown that metabolic syndrome is associated with lipid-rich plaques that contribute to the increasing risk of plaque vulnerability.¹⁸ In the present study, within the AMI group, the number of PR and LAP was significantly higher in patients with metabolic syndrome than in those without the syndrome. This finding might explain the mechanism of metabolic syndrome contributing to the increased risk of cardiovascular events.

A previous study examined the geographical distribution of occlusive thromboses throughout the coronary tree and showed that such occlusions are clustered within the proximal portions of the major epicardial arteries.¹⁹ In the present study, we observed culprit lesions and PR and LAP of non-culprit lesions in the proximal LAD of AMI patients more frequently than in other sites on CTA. The use of optical coherence tomography (OCT) revealed thin-capped fibroatheromas (TCFAs) in the proximal left coronary artery more frequently than in other sites.²⁰ The frequency of PR and LAP we observed is very similar to that of the TCFAs reported in the previous OCT study. We have shown that CTA can noninvasively reveal the PR and LAP in non-culprit lesions favoring a propensity to rapidly progress to a culprit lesion or rupture.

The largest prognostic study with thallium-201 SPECT showed a cardiac mortality rate of 0.42%/y in patients with normal scans and 2.1%/y in patients with abnormal scans.²¹ However it is not clear how many of these patients had vulnerable coronary plaques leading to ACS and cardiac events. In the present study, we showed that the number of coronary plaques in non-culprit lesions is observed significantly less frequently in SAP patients with normal MPI than in AMI patients. Specifically, calcified

plaques were more significantly observed in SAP patients with abnormal MPI than in AMI patients. The prevalence of CAD in SAP patients with normal MPI was also small, in concordance with 14 published reports comprising more than 12000 patients that showed normal stress SPECT ^{99m}Tc -sestamibi images to be associated with an average annual hard event rate of 0.6%.²²

The advantage of CTA over that of invasive modalities such as IVUS, angiography, and OCT is its noninvasive character. We noninvasively identified differences in plaque morphology and composition between non-culprit lesions in patients with AMI and SAP on CT images. The ability to noninvasively identify PR and LAP has major clinical implications because ACS represents the leading cause of morbidity and mortality worldwide. Furthermore, CTA contributes important morphologic information in addition to evaluating the functional significance of coronary stenosis with stress MPI. If confirmed by further studies, secondary prevention should be considered with intensive lipid-lowering therapy such as statin use in patients with identified PR and LAP. Indeed, early initiation of statin treatment following AMI is associated with a lower 1-year mortality rate.²³

The current study has some limitations. First, radiation dose levels to the patient are relatively high when stress MPI and CTA are combined. It is expected that radiation exposure will be significantly reduced with the use of a modified protocol that includes ECG-pulsing. Second, the threshold of 30 HU for the LAP was limited as the CT density of non-calcified plaques depends on the image quality and intraluminal contrast attenuation, and no correlation to IVUS was performed in the present study.

1. Raff GL, Gallagher MJ, O'Neill WW, Goldstein JA. Diagnostic accuracy of noninvasive coronary angiography using 64-slice spiral computed tomography. *J Am Coll Cardiol* 2005;46:552-557.
2. Sato A, Hiroe M, Tamura M, Ohigashi H, Nozato T, Hikita H, Takahashi A, Aonuma K, Isobe M. Quantitative measures of coronary stenosis severity by 64-slice computed tomography angiography and relation to physiologic significance of perfusion in non-obese patients: comparison with stress myocardial perfusion imaging. *J Nucl Med* 2008;49:564-572.
3. Leber AW, Knez A, White CW, Becker A, von Ziegler F, Muehling O, Becker C, Reiser M, Steinbeck G, Boekstegers P. Composition of coronary atherosclerotic plaques in patients with acute myocardial infarction and stable angina pectoris determined by contrast-enhanced multislice computed tomography. *Am J Cardiol* 2003;91:714-718.
4. Hoffmann U, Moselewski F, Nieman K, Jang IK, Ferencik M, Rahman AM, Cury RC, Abbara S, Joneidi-Jafari H, Achenbach S, Brady TJ. Noninvasive assessment of plaque morphology and composition in culprit and stable lesions in acute coronary syndrome and stable lesions in stable angina by multidetector computed tomography. *J Am Coll Cardiol* 2006;47:1655-1662.
5. Motoyama S, Kondo T, Sarai M, Sugiura A, Harigaya H, Sato T, Inoue K, Okamura M, Ishii J, Anno H, Virmani R, Ozaki Y, Hishida H, Narula J. Multislice computed tomographic characteristics of coronary lesions in acute coronary syndromes. *J Am Coll Cardiol* 2007;50:319-326.
6. Motoyama S, Sarai M, Harigaya H, Anno H, Inoue K, Hara T, Naruse H, Ishii J, Hishida H, Wong ND, Virmani R, Kondo T, Ozaki Y, Narula J. Computed

- tomographic angiography characteristics of atherosclerotic plaques subsequently resulting in acute coronary syndromes. *J Am Coll Cardiol* 2007;54:49-57.
7. Leber AW, Knez A, Becker A, Becker C, von Ziegler F, Nikolaou K, Rist C, Reiser M, White CW, Steinbeck G, Boekstegers P. Accuracy of multidetector spiral computed tomography in identifying and differentiating the composition of coronary atherosclerotic plaques: a comparative study with intracoronary ultrasound. *J Am Coll Cardiol* 2004;43:1241-1247.
 8. Achenbach S, Moselewski F, Ropers D, Ferencik M, Hoffmann U, MacNeill B, Pohle K, Baum U, Anders K, Jang IK, Daniel WG, Brady TJ. Detection of calcified and noncalcified coronary atherosclerotic plaque by contrast-enhanced, submillimeter multidetector spiral computed tomography: a segment-based comparison with intravascular ultrasound. *Circulation* 2004;109:14-17.
 9. Alderman EL, Stadius ML. The angiographic definitions of the Bypass Angioplasty Revascularization Investigation. *Coron Artery Dis* 1992;3:1189-1207.
 10. Cerqueira MD, Weissman NJ, Dilsizian V, Jacobs AK, Kaul S, Laskey WK, Pennell DJ, Rumberger JA, Ryan T, Verani MS. Standardized myocardial segmentation and nomenclature for tomographic imaging of the heart: a statement for healthcare professionals from the Cardiac Imaging Committee of the Council on Clinical Cardiology of the American Heart Association. *Circulation* 2002;105:539-542.
 11. Grundy SM, Cleeman JI, Daniels SR, Donato KA, Eckel RH, Franklin BA. Diagnosis and management of the metabolic syndrome: An American Heart Association/National Heart, Lung, and Blood Institute Scientific Statement. *Circulation* 2005;112:2735-2752.

12. Alberti KG, Zimmet P, Shaw J. Metabolic syndrome: A new worldwide definition. *Diabet Med* 2006;23:469-480.
13. Glaser R, Selzer F, Faxon DP, Laskey WK, Cohen HA, Slater J, Detre KM, Wilensky RL. Clinical progression of incidental, asymptomatic lesions discovered during culprit vessel coronary intervention. *Circulation* 2005;111:143-149.
14. Varnava AM, Mills PG, Davies MJ. Relationship between coronary artery remodeling and plaque vulnerability. *Circulation* 2002;105:939-943.
15. Yamagishi M, Terashima M, Awano K, Kijima M, Nakatani S, Daikoku S, Ito K, Yasumura Y, Miyatake K. Morphology of vulnerable coronary plaque: insights from follow-up of patients examined by intravascular ultrasound before an acute coronary syndrome. *J Am Coll Cardiol* 2000;35:106-111.
16. Nissen SE. Application of intravascular ultrasound to characterize coronary artery disease and assess the progression or regression of atherosclerosis. *Am J Cardiol* 2002;89:24B-31B.
17. Malik S, Wong ND, Franklin SS, Kamath TV, L'Italien GJ, Pio JR, Williams GR. Impact of the metabolic syndrome on mortality from coronary heart disease, cardiovascular disease, and all causes in United States adults. *Circulation* 2004;110:1245-1250.
18. Amano T, Matsubara T, Uetani T, Nanki M, Marui N, Kato M, Arai K, Yokoi K, Ando H, Ishii H, Izawa H, Murohara T. Impact of metabolic syndrome on tissue characteristics of angiographically mild to moderate coronary lesion integrated backscatter intravascular ultrasound study. *J Am Coll Cardiol* 2007;49:1149-1156.
19. Wang JC, Normand SL, Mauri L, Kuntz RE. Coronary artery spatial distribution of acute myocardial infarction occlusions. *Circulation* 2004;110:278-284.

20. Tanaka A, Imanishi T, Kitabata H, Kubo T, Takarada S, Kataiwa H, Kuroi A, Tsujioka H, Tanimoto T, Nakamura N, Mizukoshi M, Hirata K, Akasaka T. Distribution and frequency of thin-capped fibroatheromas and ruptured plaques in the entire culprit coronary artery in patients with acute coronary syndrome as determined by optical coherence tomography. *Am J Cardiol* 2008;102:975-979.
21. Machecourt J, Longère P, Fagret D, Vanzetto G, Wolf JE, Polidori C, Comet M, Denis B. Prognostic value of thallium-201 single-photon emission computed tomographic myocardial perfusion imaging according to extent of myocardial defect. Study in 1926 patients with follow-up at 33 months. *J Am Coll Cardiol* 1994;23:1096-1106.
22. Iskander S, Iskandrain AE. Risk assessment using single-photon emission computed tomographic technetium-99m sestamibi imaging. *J Am Coll Cardiol* 1998;32:57-62.
23. Stenestrand U, Wallentin L; Swedish Register of Cardiac Intensive Care (RIKS-HIA). Early statin treatment following acute myocardial infarction and 1-year survival. *JAMA* 2001;285:430-436.

Figure Legends

Figure 1. Sixty-four-slice CTA images of non-culprit lesions present in the three major coronary arteries in a 47-year-old man with inferior AMI. (A) Non-calcified plaques in the proximal and mid RCA and coronary stent in the culprit lesion in the distal RCA. (B) Coronary plaques in the proximal and mid LAD. (C) Non-calcified plaque in the mid LC. (D)(E) Cross-sectional images showed mild stenosis with normal CT values. (F) Cross-sectional image of plaque with low CT value (16 HU) and positive remodeling (RI: 1.10) in the proximal LAD. (G) Cross-sectional image of non-calcified plaque with low CT value (0 HU) in the mid LAD. (H) Cross-sectional image from the proximal LC showed low CT value (15 HU) and positive remodeling (RI: 1.05). (I) Cross-sectional image of non-calcified plaque in the distal LC.

Figure 2. Mean number of the coronary plaques in the non-culprit segments of the AMI and SAP patients. AMI = acute myocardial infarction; SAP = stable angina pectoris; MPI = myocardial perfusion imaging; PR = positive remodeling; LAP = low-attenuation plaques.

Figure 3. Mean total number of coronary plaques and PR and LAP in the non-culprit segments of the AMI patients with and without metabolic syndrome. Met S = metabolic syndrome; PR = positive remodeling; LAP = low-attenuation plaques.

Figure 4. Spatial distribution of the coronary plaques in the non-culprit segments of the

AMI patients. (A) Non-calcified plaques, (B) Calcified plaques, (C) PR and LAP, and (D) Mixed plaques. RCA = right coronary artery; LAD = left anterior descending artery; LC = left circumflex artery; PR = positive remodeling; LAP = low-attenuation plaques.

Table 1. Clinical Characteristics of the Patients

Variable	AMI (n = 60)	SAP with abnormal MPI (n = 67)	SAP with normal MPI (n = 83)	p Value
Age (years)	64±10	67±12	66±10	0.35
Male/female	49/11	40/12	49/34	<0.01
Hypertension	33 (55%)	37 (56%)	43 (52%)	0.85
Hyperlipidemia	30 (50%)	36 (54%)	40 (48%)	0.83
Diabetes mellitus	25 (42%)	30 (45%)	27 (33%)	0.41
Smoker	35 (58%)	34 (51%)	35 (43%)	0.23
Body mass index (kg/m ²)	24.7 (22.0-26.3)	24.4 (22.3-26.7)	23.7 (20.7-26.2)	0.50
Culprit coronary artery				0.69
Right	20	21	-	
Left anterior descending	36	43		
Left circumflex	4	3		

AMI = acute myocardial infarction

SAP = stable angina pectoris

MPI = myocardial perfusion imaging

Figure1
[Click here to download Figure\(s\): Figure 1.ppt](#)

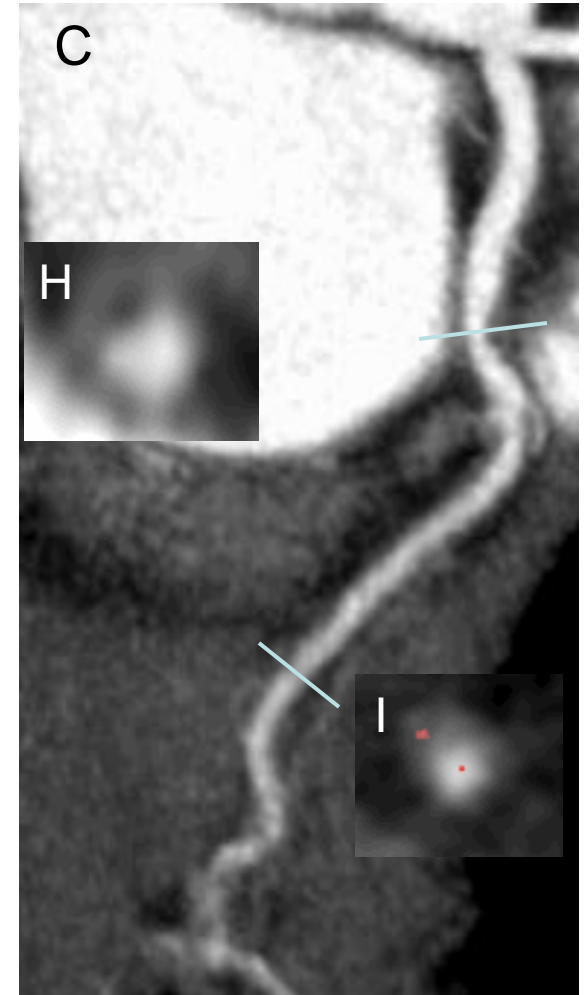
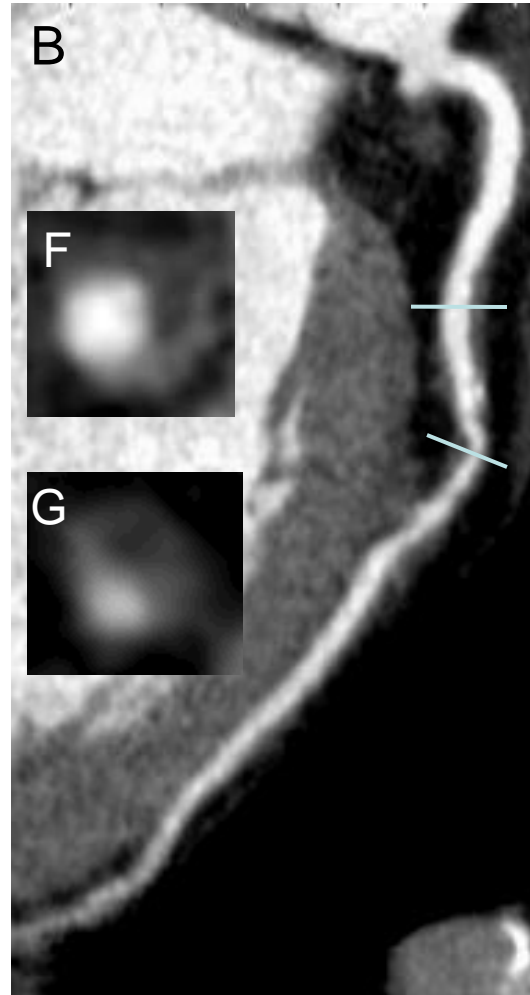
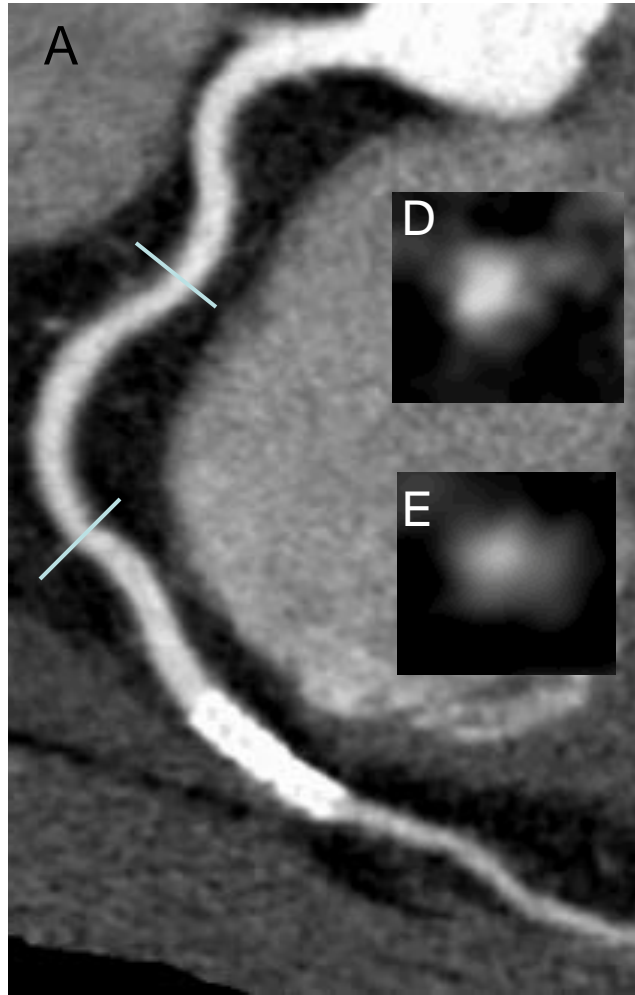


Figure2

[Click here to download Figure\(s\): Figure 2.ppt](#)

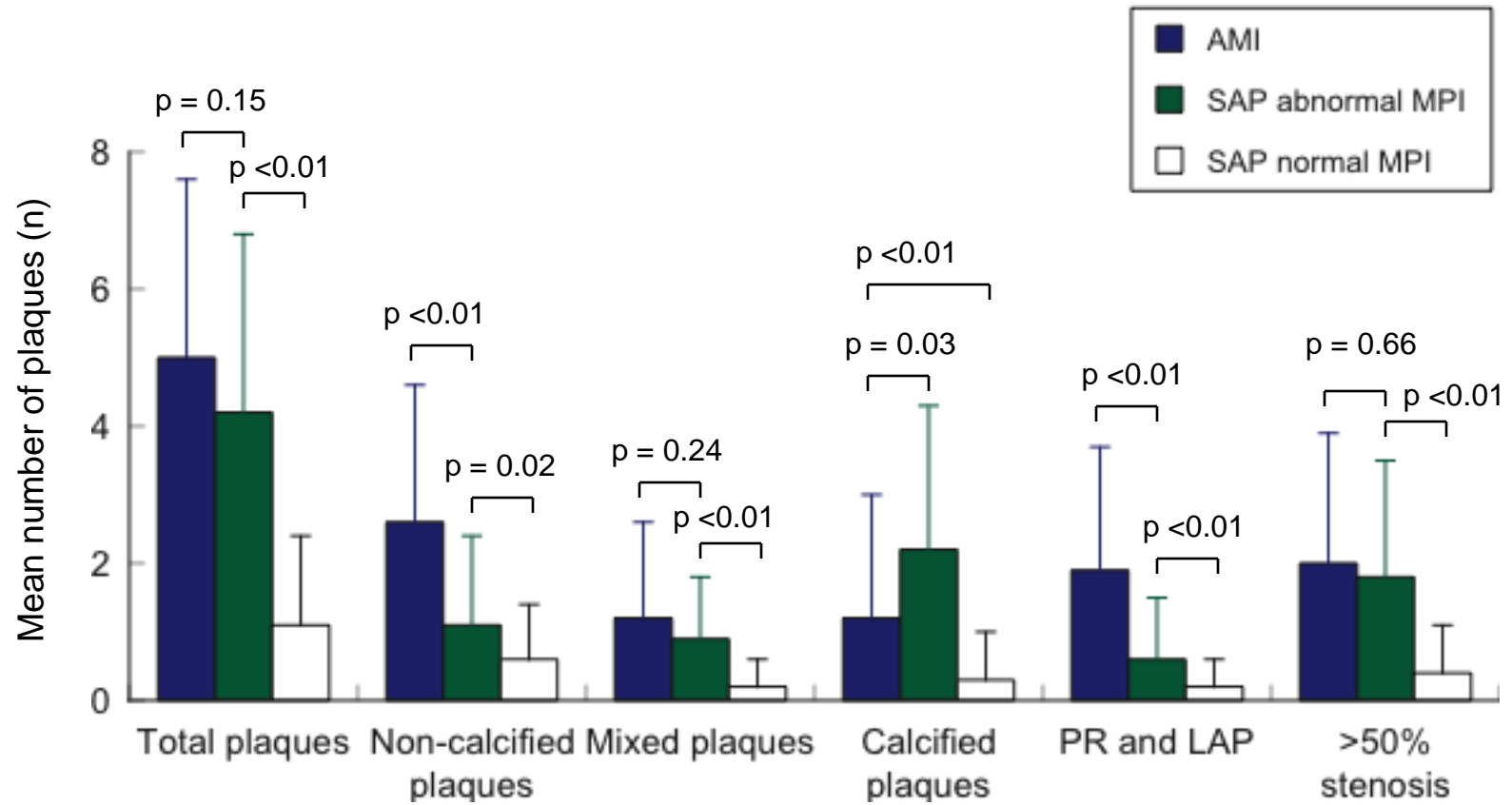


Figure3

[Click here to download Figure\(s\): Figure 3.ppt](#)

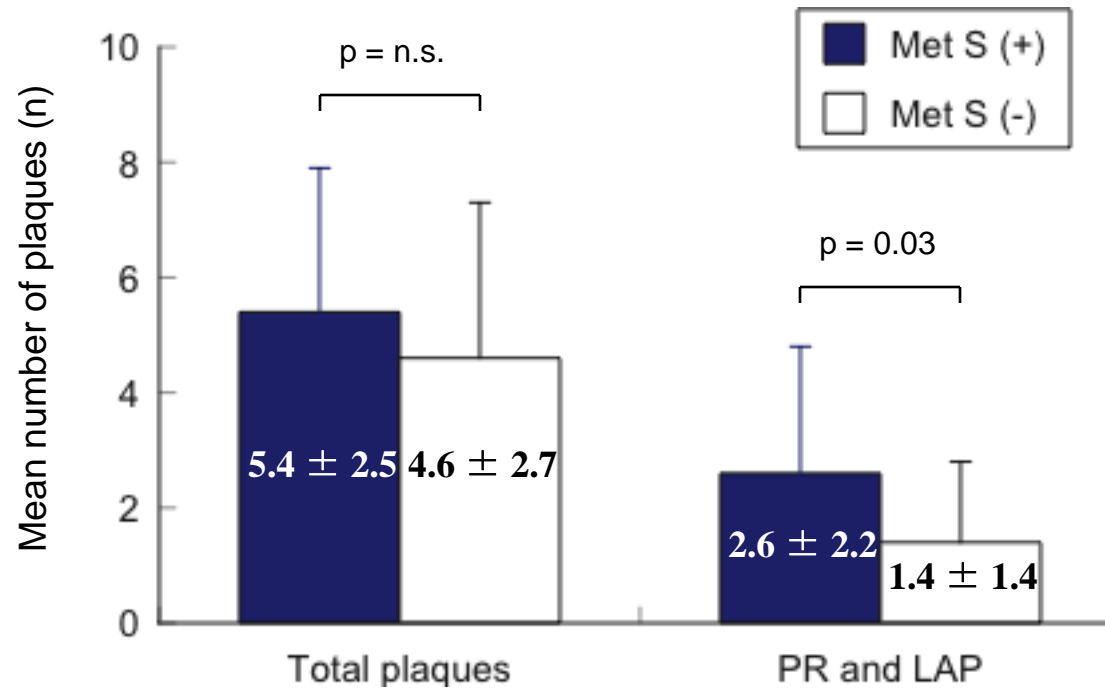


Figure 4
Click here to download Figure 4 (5) plaque.ppt

